TITLE: Evolution in *Sinocyclocheilus* cavefish is marked by rate shifts, reversals and origin of novel traits

Ting-Ru Mao†,[1], Ye-Wei Liu†, [1], Madhava Meegaskumbura†,‡, [1], Jian Yang[2], Gajaba Ellepola[1,3], Gayani Senevirathne[4], Cheng-Hai Fu[1], Joshua B. Gross[5], Marcio R. Pie[6]

[1]*Guangxi Key Laboratory for Forest Ecology and Conservation, College of Forestry, Guangxi University, Nanning, Guangxi, P.R.C.*

[2]*Key Laboratory of Environment Change and Resource Use, Beibu Gulf, Nanning Normal University, Nanning, Guangxi, P.R.C.*

[3]*Faculty of Science, University of Peradeniya, Peradeniya, KY 20400, Sri Lanka*

[4]*Department of Organismal Biology & Anatomy, University of Chicago, Chicago, IL, USA*

[5]*Department of Biological Sciences, University of Cincinnati, Cincinnati, Ohio, USA*

[6]*Departamento de Zoologia, Universidade Federal do Paraná, Curitiba, Paraná, Brazil 81531-980*

† - equal contribution

‡ - corresponding author - madhava_m@mac.com

ABSTRACT

Epitomized by the well-studied *Astyanax mexicanus*, cavefishes provide important model organisms to understand adaptations in response to divergent natural selection. However, the spectacular *Sinocyclocheilus* diversification of China, the most diverse cavefish clade in the world

harboring nearly 75 species, demonstrate evolutionary convergence for many traits, yet remain poorly understood in terms of their morphological evolution. Here, using a broad sample of 49 species representative of this diversification, we analyze patterns of *Sinocylocheilus* evolution in a phylogenetic context. We categorized species into morphs based on eye-related condition: Blind, Micro-eyed (small-eyed), and Normal-eyed and we also considered three habitat types (Troglodytic – cave-restricted; Troglophilic – cave-associated; Surface – outside of caves). Geometric morphometric analyses show Normal-eyed morphs with fusiform shapes being segregated from Blind/Micro-eyed (Eye-regressed) morphs with deeper bodies along the first principal component ("PC") axis. The second PC axis accounts for shape complexity related to the presence of horns. Ancestral character reconstructions of morphs suggest at least three independent origins of Blind morphs, each with different levels of modification in relation to the typical morphology of ancestral Normal-eyed morphs. Interestingly, only some Blind or Micro-eyed morphs bear horns and they are restricted to a single clade (Clade B) and arising from a Troglodytic ancestral species. Our geophylogeny shows an east-to-west diversification spanning the Pliocene and the Pleistocene, with Troglodytic species dominating karstic subterranean habitats of the plains whereas predominantly Surface species inhabit streams and pools in hills to the west (perhaps due to the scarcity of caves). Integration of morphology, phylogeny and geography suggests *Sinocyclocheilus* are pre-adapted for cave dwelling. Analyses of evolutionary rates suggest that lineages leading to Blind morphs were characterized by significant rate shifts, such as a slowdown in body size evolution and a 3.3 to 12.5 fold increase in the evolutionary rate of eye regression. Furthermore, body size and eye size have undergone reversals, but horns have not, a trait that seem to require substantial evolutionary time to form. These results, compared to the *Astyanax* model

system, indicate *Sinocyclocheilus* fishes demonstrate extraordinary morphological diversity and variation, offering an invaluable model system to explore evolutionary novelty.

KEYWORDS: Phylomorphospace, Evolutionary Convergence, Blind fish, Troglodytism, Geophylogeny, Pre-adaptation

INTRODUCTION

Due to the absence of light, stable mean temperatures, absence of primary productivity, and paucity of dissolved oxygen, subterranean habitats are among the most challenging environments for life on earth (Ginet and Decou, 1977, Camacho, 1992). From surface-dwelling ancestral species, cavefish have secondarily adapted to live in cave systems, often demonstrating a remarkable array of morphological and behavioral adaptations (Soares and Niemiller, 2013; Yoshizawa, 2015). These involve enhanced sensation, and also dispensing of traits that incur a developmental or energetic cost. Cavefish species can be divided into two forms: troglophiles are closely associated with caves, but do not entirely depend on them, and troglobites are obligate cave dwellers (Dowling et al., 2002; Jingcheng and Weicheng, 2015). Troglobite fish *may* harbor special adaptations, such as complete eye loss, loss of pigmentation, changes in cranial symmetry, proliferation of neuromast sensory organs, development of horns, and in some species flat, hollow heads (Strecker et al., 2004; Zhao, 2006; Gross et al., 2008). Despite the ~200 cavefish species from across the world, large diversification of cavefishes is rare. However, one extensive diversification occurs in *Sinocyclocheilus*, a monophyletic group of cyprinid fishes endemic to China, which allows a robust analysis of trait evolution relative to troglomorphism in a phylogenetic context.

69 The specialized traits cavefish bear have led them to be developed as models of evolution
70 especially with respect to adaptations to novel environments and evolutionary convergence
71 (Culver et al., 1995; Dowling et al., 2002; Jeffery, 2001; Li et al., 2008; Strecker et al., 2004;
72 Yang et al., 2016). A lion's share of knowledge on evolution and development in cavefishes has
73 come from *Astyanax mexicanus* (Mexican tetra), a species with both surface-dwelling (pigmented
74 and eyed) and cave-dwelling morphs (depigmented and blind), which can readily interbreed
75 (Borowsky, 2008). In contrast to this well-studied model system, *Sinocyclocheilus* species not only
76 include blind and normal-eyed morphs (Lan et al., 2013), but demonstrate a continuum from blind
77 to normal-eyed species. Indeed, members of the *Sinocyclocheilus* genus display remarkable
78 morphological evolution with divergent cave-dwelling, cave-associated, and surface-dwelling
79 species.

80 *Sinocyclocheilus* species are thought to have shared a common ancestor in the late Miocene,
81 undergoing a spectacular diversification spanning the Pliocene and Pleistocene across the
82 southwestern parts of China's 620,000 km^2 of karst habitats (Huang et al., 2008), with nearly 75
83 extant species (Jiang et al., 2019). This resulted in an adaptive diversification into subterranean
84 refugia traversing the intersection of the Guizhou, Guangxi and Yunnan provinces around the time
85 of the uplifting of Tibetan/Guizhou plateau (Li et al., 2008).

86 One of the most striking forms of cave adaptation in *Sinocyclocheilus* is variation in eye
87 morphology, categorized often into three morphs (Zhao and Zhang, 2009), ranging from Normal-
88 eyed to Micro-eyed (small-eyed) to Blind species. Of all Chinese hypogean fishes, 56 species show
89 troglomorphism such as reduction and/or loss of eyes, pigmentation, and the gas bladder. Presence
90 of a horn-like structure and hyper-development of the dorsal protuberance (similar to a humpback

whale) are two additional unique characters to certain Chinese hypogean species (Romero et al., 2009). These dramatic adaptations to cave life are reflected in the unique morphology of these fish.

The morphology of *Sinocyclocheilus* is most likely attributed to their habitat and local adaptations, however the precise function of certain morphologies (e.g., their horns and humps) remains unknown (Ma and Zhao, 2012). For instance, many blind species are obligate cave dwellers that have the ability to navigate along cave walls, cave-bottoms and within narrow passages (Yoshizawa, 2015). Yet, others are open water species that navigate in the manner of typical fish. There are also intermediate forms between these two principal morphs (Zhao and Zhang, 2009). However, the morphology of these fishes is so extreme that substantial variation in morphology is evident even within blind, intermediate and the open water species.

The pattern of body shape evolution in *Sinocyclocheilus* is a conundrum, which has not been addressed in an evolutionary context. Here, we explore key patterns of morphological evolution in these fishes, and demonstrate that the evolution in *Sinocyclocheilus* has been associated with significant rate changes and trait reversals across their phylogenetic history.

MATERIALS & METHODS

Phylogeny estimation

We compiled sequence data from GenBank for two mtDNA fragments (*NADH4* and *cytb*) of 39 *Sinocyclocheilus* species, and the outgroup species *Linichthys laticeps* (Cyprinidae). In addition, we generated sequence data for the *cytb* gene fragment of ten additional *Sinocyclocheilus* species (Table S1). For these species, total genomic DNA was extracted using the DNeasy Blood and Tissue Kit (Qiagen Inc., Valencia, CA) following the manufacturer's protocols. DNA was amplified in 25-μL volume reactions: 3 mM $MgCl_2$, 0.4 mM of dNTP, 1X buffer, 0.06 U of Taq

DNA Polymerase, 2 mM of each primer. Thermocycling conditions included an initial step at 94 °C for 3 min, followed by 35 cycles at 45 s at 94 °C, 1 min at 46-50 °C and 45 s at 48-56 °C, and a final step at 72 °C for 5 min. PCR products were electrophoresed in a 1.5% agarose gel, stained with ethidium bromide and visualized under UV light. Successfully amplified products were purified using MicroconTM Centrifugal Filter Units (Millipore, Billerica, MA, U.S.A.). Sequencing reactions were carried out in 10 µl solutions including the following final concentrations: 5 ng/µl of template DNA, 0.5 µl of Big DyeTM (Applied Biosystems Inc., Foster City, CA, U.S.A.), 0.2 µM of each primer and 0.1X of reaction buffer. The final product was purified using SephadexTM G-50 (GE Healthcare Bio-Sciences AB, Uppsala, Sweden) for sequencing. Forward and reverse strands were reconciled using Staden v.1.6.0 (Staden, 1996). Sequences from both genes were concatenated and aligned unambiguously using CLUSTALW (Thompson et al., 2003), as implemented in MEGA v. 6.0 (Tamura et al., 2013), for a total alignment length of 2155 bp. We used JMODELTEST v.2.1.10 (Santorum et al., 2014) to determine the best models of evolution for each fragment, which were implemented in BEAST v.1.10.4 (Drummond and Rambaut, 2007) as a partitioned analysis to estimate the phylogenetic relationships and relative divergence times within *Sinocyclocheilus*. We calibrated the tree using the relative time period which diversification of *Sinocyclocheilus* initiated around 11.31 Mya, a reference point obtained from (Chen et al., 2018). We used a strict molecular clock and a calibrated Yule tree prior, as well as a GTR+I+G for each partition and ran the analysis for 20 million generations using the Cipres Science Gateway Server (Miller et al., 2010). Convergence was assessed by inspecting the log-output file in TRACER v.1.6 (Drummond et al., 2012), and by ensuring ESS values were above 200. The first 10% of the trees were discarded, and the post burn-in trees were used to infer the maximum clade credibility tree using TREEANNOTATOR v.1.4.4

(Rambaut and Drummond， 2019). The maximum clade credibility tree, as well as a set of 1000 post burn-in topologies, were retained for further analyses (see below).

Morphometric data acquisition and analyses

We assembled a database of images of referenced specimens of *Sinocyclocheilus* from scaled photographs, which was complemented by species that we photographed (Table S2). The final dataset included 90 images (54 from species descriptions and catalogues and 36 from photographs by the authors) for 50 species, which included 70% of the total number of described species for the genus. These images were used for geometric morphometrics analyses, which were based on 15 landmarks (See Fig. 1A) and 180 sliding semi-landmarks, obtained using tpsDig v. 2.16 (Rohlf, 2010). Semi-landmarks were collected as curves outlining the body. These data were subsequently reduced to equidistant landmarks, and defined as semi-landmarks using tpsUtil v. 1.46 (Rohlf, 2010). We then slid the landmarks using the bending energy method (Gunz & Mitteroecker, 2013) implemented in GEOMORPH v.3.2.0 (Adams & Otárola-Castillo, 2013). The landmark coordinates were aligned using a generalized Procrustes superimposition analysis (Adams et al., 2013), and a principal component analysis (PCA) was used to evaluate shape variation within the sample.

Multiple images for the same species were used to obtain the landmarks and the mean of their Procrustes coordinates were calculated to be used in later analyses. We also obtained traditional linear measurements, namely standard length (SL), eye diameter (ED) and standardized eye diameter (sED, calculated as the ratio between ED and SL).

Morphological and habitat evolution

159 Since shape variation in *Sinocyclocheilus* cavefishes occurs mostly in the anterior end of the
160 fish and as one of the major features leading to this is eye-related, we considered the absence or
161 the size of the eye (when present) as a proxy for the categorization of morphs. Since the eye size
162 has an allometric association with body size, we used the standardized eye diameter (sED) in
163 placing them into three morphological categories: Blind (eye absent); Micro-eyed (0.0 – 3.0mm);
164 Normal-eyed (< 3.0mm) respectively. For ease of discussion, we considered Blind and Micro-eyed
165 together as Regressed-eyed; Micro-eyed and Normal-eyed together as Eyed species.
166 *Sinocyclocheilus* were also categorized based on their habitat as Troglodytic, Troglophilic,
167 and Surface species. Troglodytic species live in an obligatory association with caves, and are not
168 sampled outside of caves. Caves, as meant here represent roofed-caves, submerged caves, and
169 subterranean waterways that form windows intermittently with the surface. Troglophilic species
170 live in a close association with caves and are sampled both in the vicinity of cave entrances and
171 within caves. Finally, Surface species are found in habitats even when a cave is not found in close
172 proximity and live in normal streams ponds and lakes as typical fish do, but they could venture
173 into caves (underground water bodies) during unfavorable periods, when water is only available
174 in caves. It should be noted here that this categorization is strictly habitat based and not
175 morphology based (for instance, there are Normal-eyed species that are Troglodytic, Troglophilic
176 or Surface). These habitat associations are based on published literature (Zhao and Zhang, 2009;
177 Romero et al., 2009) and personal observations as outlined in Table S1.
178 To infer the number and timing of evolutionary shifts within eye-related morphs, horn
179 distribution and the habitat type, we used stochastic character mapping (Nielsen, 2002;
180 Huelsenbeck et al. 2003), as implemented in the make.simmap function in PHYTOOLS. On each of
181 the 1000 post burn-in trees obtained from BEAST, we used stochastic character mapping to

182 generate 100 potential histories. This approach therefore considers uncertainty both in the
183 evolutionary history of the traits as well as in the inferred topology of the phylogeny.

184 The landmark coordinates obtained were aligned using a generalized Procrustes
185 superimposition analysis (Adams et al., 2013), and a principal component analysis (PCA) was used
186 to explore shape variation within the sample. In addition, we described the eye-related
187 morphological variation in *Sinocyclocheilus* by estimating ancestral states of SL and ED and
188 visualizing them using traitgrams (Evans et al., 2009) as implemented in the phenogram function
189 in PHYTOOLS 0.7.20 (Revell, 2012) using the maximum clade credibility tree. We also visualized
190 the evolution of both traits simultaneously using a phylomorphospace (a projection of the tree into
191 morphospace, *sensu* Sidlauskas, 2008) using the phylomorphospace function in PHYTOOLS.

192

193 *Evolutionary rate variation in eye related morphs*

194 We tested whether the evolutionary rates of the studied continuous traits (SL, ED, sED) are
195 significantly different in different morphs. We used 100 potential trait histories from stochastic
196 character mapping and then fit two alternative models of evolution on each studied trait, one that
197 fixes the rate of evolution to be identical between morphs against an alternative model in which
198 the morphs have separate rates. We calculated the Akaike Information Criterion for small sample
199 size (AICc) from the maximum likelihood estimate on each tree using the brownie.lite function in
200 PHYTOOLS. Finally, if a multi-rate model provided a better fit to the data, we calculated model-
201 averaged estimates of evolutionary rates for each morph. Unless otherwise indicated, all analyses
202 were conducted using R v. 3.6.0 (R Core Team, 2019).

203

204 *Geophylogeny analyses*

We could not carry out a formal biogeographical analysis, given that their high endemism and the complex pattern of underground connections between caves limits the establishment of reasonable biogeographical areas. However, we assessed the geographical structuring of *Sinocyclocheilus* diversification by building a geophylogeny on GenGIS v. 2.5.3 (Parks et al., 2013) based on the maximum credibility tree.

RESULTS

The maximum credibility tree of *Sinocyclocheilus* is shown in Fig. 2 together with the reconstruction of ancestral states for eye-related morphs; we consider four major clades (A,B,C,D), as previously reported by other authors (Zhao and Zhang, 2009). Despite the inherent uncertainty in ancestral state reconstructions, it is clear that Blind species evolved at least three times in *Sinocyclocheilus*. Two of these events involved single species evolving from Normal-eyed ancestors, namely *S. xunlensis* and *S. anophthalmus*. On the other hand, the third lineage of blind *Sinocyclocheilus,* Clade B, includes several closely related species of Blind, Micro-eyed and a few Normal-eyed species, with two cases of reversal from either Micro-eyed or Blind to Normal-eyed morphs, namely *S. zhenfengensis* and *S. brevibarbatus* (Fig. 2). All four clades contain Regressed-eyed species and comparatively, clade Blind contains the most cases. Interestingly, clade B originated around the time of the beginning of the aridification process in China in the late Pliocene, whereas the other two transitions to blind species were much more recent (Fig. 2).

Interestingly, the evolution of body size and eye diameter seem to have often involved reversals, with little correspondence between body size (Fig. 3A) or eye diameter (Fig. 3B) and their corresponding morphs, except for the case of blind species for which eye diameter is necessarily zero. On the other hand, morphs are clearly distinguished when eye diameter and body

size are visualized simultaneously (Fig. 3C), which suggests that the evolution of different morphs is achieved by altering the relationships between body size and eye diameter. Habitat associations traced on the phylomorphospace (Fig. 3D) indicates that species with regressed eyes and small-to-medium body sizes are obligate cave dwellers. However, normal eyed species can be Troglodytic, Troglophilic or surface dwellers regardless of their body size. Interestingly, all horned species are obligate cave dwellers while all cave species are not horned (Fig. 3E).

A more precise description of the overall changes associated with different morphs can be visualized in the projections build from the geometric morphometrics analyses (Fig. 1B). The first PC, which accounted for approximately 32% of the variance in the dataset (see Table S3), tended to distinguish the slender Normal-eyed species on the left and Micro/Blind species on the right, which were characterized by changes in shape and widening of the anterior dorsal area between mouth and beginning of the dorsal fin of their body, resulting in a shift from the fusiform shape of the Normal-eyed forms to a more "boxy" form of the Micro-eyed and Blind forms. The second PC, which explained approximately 17% of the variance in the dataset, emphasized the differences in the type of dorsoventral broadening of the mid-section between morphs, with a shortening of the tail region (Fig. 1B). The variation in this axis is very high among the Micro-eyed and Blind forms when compared to the Normal morphs.

The multiple-rate model of evolution provided the best fit to the data for all three quantitative traits (ΔAIC=2.7, 10.7 and 7.9 respectively for ED, sED and SL; Table 1), indicating that the evolution of different *Sinocyclocheilus* morphs was associated with significant changes in their evolutionary rates. However, there were intriguing differences between traits in their rates (Table 2). The rates of evolution of eye diameter and standardized eye diameter were similar between

Normal-eyed and Micro-Eyed species, but increased between 3.3 to 12.56 times during shifts towards Blind species.

Geophylogeny represents the phylogeny overlaid across the geographic location of each species, where phylogenetic clustering is evident across the landscape. Considering the distribution of *Sinocyclocheilus,* we mainly see a pattern where the basal, Normal-eyed morphs are placed in the east, a substantial portion of Blind/Micro-eyed (Regressed-eyed) species are in the center, and Normal-eyed morphs are predominant towards the western mountains (Fig. 4).

DISCUSSION

Habitat utilization in context of eye-morphology

Integrating evolution of eye size and habitat manifests interesting and previously unrecognized evolutionary patterns in the evolution of *Sinocyclocheilus*. The Eye-size based ancestral reconstruction suggests the base of the phylogeny is most likely an Eyed species (i.e. Normal- or Micro-), but habitat reconstructions places, with high probability, Troglodytic species at the base (Fig. S1). This suggests an ancestral Eyed-species evolved a Troglodytic habit before they became blind. This may be an example of preadaptation in *Sinocyclocheilus*, i.e., the advancement of a functional change with little or no evolutionary modification (Ardila, 2016). In *Astyanax* cavefish, surface-dwelling forms are scotophilic, they prefer to remain away from direct light suggesting that scotophilia may be preadaptive for colonizing the dark, cave environment (Espinasa et al., 2001). In *Sinocyclocheilus*, since a basal (eyed) species demonstrated preference for the cave habitat, this preadaptation to darkness may hint towards why certain species tend to become cave-dwellers while others do not. This pattern is supported by two principal lines of evidence. First, most of the basal species are eyed, and Troglodytic (except for one species with

an unusual eye-related polymorphic condition that we discuss below). Second, the most westward group (Clade D; Normal-eyed Surface fish), re-colonized caves whenever cave habitats were available within that area, suggesting a strong predisposition for cave-dwelling across all *Sinocyclocheilus*. In other words, when caves were present, members of *Sinocylocheilus,* irrespective of eye-related condition, preferred the cave habitat.

The preference for caves may not be a preference for darkness, but in fact a preference for depth, in search of water for survival. In a karstic environment where drying of surface running water is common, a preference for such deeper habitats may have provided an evolutionary advantage. In the presence of an array of subterranean waterways, such a predisposition would have given rise to the eye-regressed forms living close to, or associated with, caves that are characteristic of the genus.

Furthermore, apart from the Troglodytic and Troglophilic species of Clade D, some of the putative Surface species of Clade D are often observed at the entrances of caves or at windows to subterranean rivers (Zhao and Zhang, 2009). Hence, with more intensive ecological studies, some species recognized as Surface species may indeed be Troglophilic species, bolstering the notion that *Sinocyclocheilus* are predisposed to seek deeper waters of the karstic caves.

Resource utilization plays a key survival role in harsh environments (Culver and Pipan, 2009). Some of the Troglophilic, eyed-species are nocturnal, emerging from submerged caves, presumably to feed at night to reduce competition from other non-cave inhabiting fish species (personal observations). Some species like *S. altishoulderus, S. donglanensis* (Romero et al., 2009), *S. bamaensis* (Su et al., 2003), *S. malacopterus* (Chen et al., 2017) and *S. longibarbatus* (personal observation, video evidence as Supplementary information); are known to come out of caves during the high water season, presumably to feed and breed. This explains dependence on the cave

296 as a diurnal refugium, from where these species can exploit the surface habitats at night. Strategies
297 such as this, where multiple resources are utilized simultaneously, points to the adaptability of
298 some *Sinocyclocheilus* species, resulting in their evolutionary success in a harsh and changing
299 environment. Hence, the cave entrances are possibly an important ecotone that is important in
300 *Sinocyclochelius* diversification and conservation.

301 Season and time of day seem to be important factors in determining habitat utilization patterns,
302 but this level of resolution in habitat data is not currently available for a majority of the species to
303 carry out a comprehensive habitat analysis across the diversification – indeed, many species are
304 known only from one or a few specimens (Zhao and Zhang, 2009).

305

306 ***Adaptations in the light of geophylogeny***

307 In combination with the data analyzed, basal *Sinocyclocheilus* (Clade A) are Normal-Eyed,
308 predominantly cave dwelling and non-horned species from the Eastern region of their distribution.
309 As pointed out, this suggests that the earliest ancestors of *Sinocyclocheilus* species where Normal-
310 eyed and but still lived in close association with caves. The ancestral reconstructions suggest that
311 the affinity to caves would have evolved early and is present in most *Sinocyclocheilus.* The clade
312 comprising basal species are from the east of the *Sinocyclocheilus* distribution, i.e. the He Jiang
313 and Gui Jiang river basin in northeastern Guangxi, and hence, it seems that the diversification of
314 these fish occurred from East to West (Fig. 4).

315 Within this predominantly Normal-eyed clade (Clade A), there is an exception,
316 *Sinocyclocheilus guanyangensis*, a species that we coded as Micro-eyed, has Normal-Eyed, Micro-
317 eyed and effectively Blind morphs within the same population – polymorphic for this trait. But
318 these blind morphs have their eyes completely covered by skin and the Micro-eye is not itself

319 degenerate. This kind of condition has been noted in several other taxa also (*S. xunlensis* and *S.*
320 *flexuodorsalis* – not available for our analysis), but is uncommon. This suggests a degree of
321 polymorphism for this trait, suggesting that the earliest ancestors of *Sinocyclocheilus* may have
322 been able to lose or gain eyes relatively easily as an adaptation to local conditions, this ability
323 appears several times within this cave-driven diversification.

324 The major adaptation for cave dwelling evolves predominantly in the expansive karstic area
325 in northwestern Guangxi (associated with the Liu Jiang basin and Hongshui river basin joining the
326 main Xijiang River system from the North), in Clade B, the southeastern corner of Guizhou
327 province (upper reaches of Hongshui River) and the northeastern plateau of Yunnan province. This
328 region can be considered the center for novel adaptations for *Sinocyclocheilus,* where these fishes
329 express their full morphological diversity, blindness, micro-eyedness, and their remarkable horns.
330 In the shape-related analyses, these species cluster on the right of morphospace (Fig. 1B). The
331 deeper caves and extensive subterranean river system associated with the Guangxi plains (Zhao
332 and Zhang, 2009) would have facilitated this extensive adaptive diversification (Fig. 4).

333 The karstic northwestern region that the Guangxi-dominated Clade (Clade B) experiences
334 drought conditions during much of the year, and one of the major sources of rain for the region is
335 through storms sweeping from the southeast that are strong enough to persist through the vast
336 plains of Guangxi, mainly from April to August (Zhao and Zhan, 2009). During unfavorable
337 periods, these fishes seem to have found refuge in the subterranean caves. The morphologically
338 most diverse clade being present in the region where the climatic conditions are most unfavorable
339 for surface fish, reinforces the notion that *Sinocyclocheilus* species adapted to life in caves as
340 climatic refuges (Zhao and Zhang, 2009).

341 The distribution of Clade C, characterized by mostly Normal-eyed but Troglodytic species
342 largely overlaps Clade B. In Clade C, the single Blind species (*S. xunlensis*) and the two Micro-
343 Eyed species (*S. cyphotergous* and *S. multipunctatus*) are shown within a narrow geographic area
344 on the Liu Jiang and Hongshui river system (Fig. 4).

345 Species in the clade that is found in the west (Clade D), predominantly on the hilly terrain of
346 Yunnan plateau, are predominantly Normal-eyed Surface species lacking horns (Fig. 1, Fig. 4).
347 However, wherever there are cave habitats and subterranean river systems, some of these putative
348 surface species have become facultative or obligate cave species. The obligate cave species found
349 within the region, *S. anophthalmus*, is blind. However, this Blind species stands clustered with the
350 Normal-eyed morphs in the morphospace, signifying that the shape of the species has not
351 extensively changed, possibly due to recent (Pleistocene) invasion of the cave habitat from a
352 Normal-eyed ancestor (Fig. 2) – time since becoming blind is not been long enough for change
353 into the box-like shape of the Blind species of Clade B.

354 Horn distributions show several peculiar trends. In most *Sinocyclocheilus* species, a prominent
355 hump is present (He et al., 2013). However, this hump is markedly low in the Normal-eyed surface
356 inhabiting species of the Yunnan clade (Fig. 4). For the species that bears a horn, the horn
357 represents the region in which the dorso-frontal hump is present, and always occurs before the
358 hump begins, at the boundary of the edge of the dorsal skull. The exception to this is *S.*
359 *cyphotergous* (Clade C), where a horn like structure is placed on top of the hump. *S. cyphotergous,*
360 a species found in clade C, is phylogenetically separate from other horned species, suggesting that
361 the origins of the "horn" for this species is evolutionarily different from the other horned species
362 (Fig. S2). Though the function of the horn remains unknown (protection of head, anchoring in
363 strong current and protection of head has been suggested; Zhao and Zhang, 2009), functionally

364 this structure may be similar to other species, if it is actually anchoring in strong current is the
365 main function.

366 The rates of evolution of various traits show some incongruent (non-allometric), but
367 interesting patterns that can be explained in the context to adaptations to a Troglodytic condition.
368 The rates of evolution in eye diameter are similar between Normal- and Micro-Eyed species but,
369 increases dramatically (3.3-12.56 times) with shifts towards blind forms. However, body size
370 evolution for these morpho groups shows a reversed pattern, with a 0.03 decrease in body size
371 evolution in the Blind morphs compared to the eyed-morphs. These patterns in rate variation
372 suggest that the evolution of Blind morphs to a Troglodytic habitat were simultaneously associated
373 with an increase in the rate of evolution of the eye-size degeneration and a decrease in the rate of
374 body size evolution. The smaller body size resulting from a sluggish rate of change will facilitate
375 both navigation within constricted spaces and sustenance on a limited supply of resources expected
376 to be experienced in subterranean habitats.

377 Much of our collective knowledge of the patterns and mechanisms of regressive evolution
378 come from studies of animals that have colonized the subterranean biome. Within this group, a
379 several studies have focused on the Mexican tetra, *Astyanax mexicanus* (Jeffery, 2009). This
380 natural animal model system comprises multiple cave-adapted morphs and a surface-dwelling
381 morph that resides in near the caves themselves (Gross, 2012). Since the discovery of *Astyanax*
382 cavefish in 1936, countless studies have provided insight to the developmental and genetic bases
383 for cave-associated traits (Hubbs and Innes, 1936). Indeed, much of this insight has emerged from
384 the interbreeding studies of conspecific cave and surface morphs (reviewed in Wilkens, 2016).
385 However, several aspects of regressive evolution and troglomorphic adaptation remain unresolved.
386 Owing to several of the differences with *Astyanax*, we argue that *Sinocyclocheilus* is well-

387 positioned to provide important new insights to broader patterns of diversification and adaptation
388 in cave-dwelling organisms.

389 For instance, *Astyanax* represents a single species with 30 different interfertile populations
390 from a relatively small geographic location (Wilkens and Strecker, 2017). In contrast,
391 *Sinocyclochelius* harbors about 75 species (49 in our study) inhabiting diverse geographic biomes
392 across a much larger geographic area. Moreover, while *Astyanax* cavefish converge on similar
393 phenotypes (regressed vision and pigmentation), they are not regarded as having numerous
394 morphological novelties. In contrast, *Sinocyclocheilus* species have recurrently evolved a unique
395 "horn" (Soares et al., 2019) from several eyeless species. Similarly, the larger number of
396 *Sinocyclocheilus* species allows keener resolution for understanding broad phylogenetic processes,
397 such as trait reversals and directions of diversification. Although a reversal from an eyeless to an
398 eyed form has been reported for one cave population in *Astyanax* (Caballo Moro; Krishnan and
399 Rohner, 2017), this phenomenon appears to be much less common than in *Sinocyclocheilus*.
400 Additionally, a clear polarity of diversification is lacking in *Astyanax* cavefish, rather ancient
401 stocks of surface-dwelling forms appear to have recurrently invaded caves to the east (i.e., Sierra
402 de El Abra caves), with more recent invasions having occurred in the northern (Sierra de Colmena)
403 and the western caves (Sierra de Guatemala; Bradic et al., 2012). However, the well-characterized
404 gene flow between the cave and surface waters obscures the ability to understand clear boundaries
405 between different cave groups. Further, most *Astyanax* cave populations are believed to have
406 diverged over the course of the last ~200 – 500 Ky (Herman et al., 2018). By contrast,
407 *Sinocyclocheilus* species are much older, and therefore one can determine how longer-term
408 processes unfold in these cave-dwelling animals. Thus, despite clear phylogenetic differences

409 between *Astyanax* and *Sinocyclocheilus*, both genera have the ability to provide complementary
410 and critical insights to the processes underlying cave evolution and diversification.

411 The integration of morphology, phylogeny, rate analyses, dating and distribution show not
412 only several remarkable patterns of evolution, but also interesting exceptions to these patterns that
413 signifies the diversification of *Sinocyclocheilus* as a unique model system to study evolutionary
414 novelty.

415

416 ## ACKNOWLEDGEMENTS

417 We thank the following institutions and individuals: funding from Guangxi University Special
418 Talent Recruitment Grant to MM; funding from National Natural Science Foundation of China
419 (31860600 and Guangxi Natural Science Foundation (2017GXNSFFA198010) JY; Shipeng Zhou,
420 Bing Chen, Dan Sun, Jayampathi Herath and Amrapali Rajput for assistance in the field; Ethical
421 review approval from Guangxi University.

422

423 ## REFERENCES

424 Adams, D. C., and E. Otárola-Castillo. 2013. geomorph: an r package for the collection and
425 analysis of geometric morphometric shape data. Methods Ecol Evol 4:393–399.

426 Adams, D. C., F. J. Rohlf, and D. E. Slice. 2013. A field comes of age: geometric morphometrics
427 in the 21st century. Hystrix, the Italian Journal of Mammalogy 24:7–14.

428 Ardila, A. 2016. The Evolutionary Concept of "Preadaptation" Applied to Cognitive
429 Neurosciences. Front. Neurosci. 10:103.

430 Borowsky, R. 2008. Breeding *Astyanax mexicanus* through Natural Spawning. Cold Spring
431 Harbor Protocols 2008:pdb.prot5091-pdb.prot5091.

Bradic, M., P. Beerli, F. J. García-de León, S. Esquivel-Bobadilla, and R. L. Borowsky. 2012. Gene flow and population structure in the Mexican blind cavefish complex (*Astyanax mexicanus*). BMC Evol Biol 12:9.

Camacho , A. I. ed. 1992. The Natural History of Biospeology. Monographs of the National Museum of Natural Sciences. . National Museum of Natural Sciences., Madrid.

Chen, Y.-Y., R. Li, C.-Q. Li, W.-X. Li, H.-F. Yang, H. Xiao, and S.-Y. Chen. 2018. Testing the validity of two putative sympatric species from *Sinocyclocheilus* (Cypriniformes: Cyprinidae) based on mitochondrial cytochrome b sequences. Zootaxa 4476:130.

Chen, Z. M., J. Luo, H. Xiao, and J. X. Yang. 2010. Subterranian fishes of China. Pp. 397–414 *in* Biology of Subterranean Fishes. E. Trajano, M. E. Bichuette, B.G. Kapoor (eds）. Science Publishers, USA.

Culver, D. C., T. C. Kane, and D. W. Fong. 1995. Adaptation and natural selection in caves: the evolution of Gammarus minus. Harvard University Press, Cambridge, Mass.

Culver, D. C., and T. Pipan. 2009. The biology of caves and other subterranean habitats. Oxford University Press, New York.

Dowling, T. E., D. P. Martasian, and W. R. Jeffery. 2002. Evidence for Multiple Genetic Forms with Similar Eyeless Phenotypes in the Blind Cavefish, *Astyanax mexicanus*. Molecular Biology and Evolution 19:446–455.

Drummond, A. J., and A. Rambaut. 2007. BEAST: Bayesian evolutionary analysis by sampling trees. BMC Evol Biol 7:214.

Drummond, A. J., M. A. Suchard, D. Xie, and A. Rambaut. 2012. Bayesian Phylogenetics with BEAUti and the BEAST 1.7. Molecular Biology and Evolution 29:1969–1973.

454 Espinasa, L., P. Rivas-Manzano, and H. E. Pérez. 2001. A New Blind Cave Fish Population of
455 Genus *Astyanax*: Geography, Morphology and Behavior. Environmental Biology of Fishes
456 62:339–344.
457 Evans, M. E. K., S. A. Smith, R. S. Flynn, and M. J. Donoghue. 2009. Climate, Niche Evolution,
458 and Diversification of the "Bird-Cage" Evening Primroses (*Oenothera* , Sections *Anogra*
459 and *Kleinia*). The American Naturalist 173:225–240.
460 Ginet, R., and V. Decu. 1977. Initiation à la biologie et à l'écologie souterraines. J.-P. Delarge,
461 Paris.
462 Gross, J. B. 2012. The complex origin of *Astyanax* cavefish. BMC Evol Biol 12:105.
463 Gross, J. B., M. Protas, M. Conrad, P. E. Scheid, O. Vidal, W. R. Jeffery, R. Borowsky, and C. J.
464 Tabin. 2008. Synteny and candidate gene prediction using an anchored linkage map of
465 *Astyanax mexicanus*. Proceedings of the National Academy of Sciences 105:20106–20111.
466 Gunz, P., and P. Mitteroecker. 2013. Semilandmarks: a method for quantifying curves and
467 surfaces. Hystrix, the Italian Journal of Mammalogy 24(1):103-109.
468 He, Y., X. Y. Chen, T. Q. Xiao, and J. X. Yang. 2013. Three-dimensional morphology of the
469 *Sinocyclocheilus hyalinus* (Cypriniformes: Cyprinidae) horn based on synchrotron X-ray
470 microtomography . Zoological Research 34(4−5):128–134.
471 Herman, A., Y. Brandvain, J. Weagley, W. R. Jeffery, A. C. Keene, T. J. Y. Kono, H. Bilandžija,
472 R. Borowsky, L. Espinasa, K. O'Quin, C. P. Ornelas-García, M. Yoshizawa, B. Carlson, E.
473 Maldonado, J. B. Gross, R. A. Cartwright, N. Rohner, W. C. Warren, and S. E. McGaugh.
474 2018. The role of gene flow in rapid and repeated evolution of cave-related traits in Mexican
475 tetra, *Astyanax mexicanus*. Mol Ecol 27:4397–4416.

476 Huang, Q., Y. Cai, and X. Xing. 2008. Rocky Desertification, Antidesertification, and
477 Sustainable Development in the Karst Mountain Region of Southwest China. AMBIO: A
478 Journal of the Human Environment 37:390–392.
479 Hubbs, C. L., and W. T. Innes . 1936. The first known blind fish of the family Characidae: A
480 new genus from Mexico. Occasional papers of the Museum of Zoology, University of
481 Michigan 342:1–10.
482 Huelsenbeck, J. P., R. Nielsen, and J. P. Bollback. 2003. Stochastic Mapping of Morphological
483 Characters. Systematic Biology 52:131–158.
484 Jeffery, W. R. 2001. Cavefish as a Model System in Evolutionary Developmental Biology.
485 Developmental Biology 231:1–12.
486 Jeffery, W. R. 2009. Regressive evolution in *Astyanax* cavefish. Annual Review of Genetics
487 43:25–47.
488 Jiang, W. S., J. Li, X. Z. Lei, Z. R. Wen, Y. Z. Han, J. X. Yang, and J. B. Chang. 2019.
489 *Sinocyclocheilus sanxiaensis*, a new blind fish from the Three Gorges of Yangtze River
490 provides insights into speciation of Chinese cavefish. Zoological research 40(6):552–557.
491 Jingcheng, R., and Y. Weicheng. 2015. A Review of Progress in Chinese Troglofauna Research.
492 Journal of Resources and Ecology 6:237–246.
493 Krishnan, J., and N. Rohner. 2017. Cavefish and the basis for eye loss. Phil. Trans. R. Soc. B
494 372:20150487.
495 Lan, J. H., X. Gan, T. J. Wu, and J. Yang. 2013. Cave fishes of Guangxi, China. Science Press,
496 Beijing.
497 Li, Z., B. Guo, J. Li, S. He, and Y. Chen. 2008. Bayesian mixed models and divergence time
498 estimation of Chinese cavefishes (Cyprinidae: *Sinocyclocheilus*). Sci. Bull. 53:2342–2352.

499 Lunghi, E., Y. Zhao, X. Sun, and Y. Zhao. 2019. Morphometrics of eight Chinese cavefish
500 species. Sci Data 6:233.
501 Ma, L. and Y.H. Zhao. 2012. Cavefish of China. in: White, W.B.; and D.C. Cuvier, editors.
502 Encyclopedia of Caves. Pp. 107—125 Elsevier. ISBN 9780123838322
503 Miller, M. A., W. Pfeiffer, and T. Schwartz. 2010. Creating the CIPRES Science Gateway for
504 inference of large phylogenetic trees. Pp. 1–8 *in*. New Orleans, LA.
505 Nielsen, R. 2002. Mapping Mutations on Phylogenies. Systematic Biology 51:729–739.
506 Parks, D. H., T. Mankowski, S. Zangooei, M. S. Porter, D. G. Armanini, D. J. Baird, M. G. I.
507 Langille, and R. G. Beiko. 2013. GenGIS 2: Geospatial Analysis of Traditional and Genetic
508 Biodiversity, with New Gradient Algorithms and an Extensible Plugin Framework. PLoS
509 ONE 8:e69885.
510 R Development Core Team. 2019. a language and environment for statistical computing:
511 reference index. R Foundation for Statistical Computing, Vienna.
512 Rambaut, A., and A. J. Drummond. 2013. TreeAnnotator v1.10.4. Available as part of the
513 BEAST package at http://beast.bio.ed.ac.uk. .
514 Revell, L. J. 2012. phytools: an R package for phylogenetic comparative biology (and other
515 things): phytools: R package. Methods in Ecology and Evolution 3:217–223.
516 Rohlf, F. J. 2010. tpsDig 2.16 edn. at http://life.bio.sunysb.edu/morph/.
517 Romero, A., Y. Zhao, and X. Chen. 2009. The Hypogean fishes of China. Environ Biol Fish
518 86:211–278.
519 Santorum, J. M., D. Darriba, G. L. Taboada, and D. Posada. 2014. jmodeltest.org: selection of
520 nucleotide substitution models on the cloud. Bioinformatics 30:1310–1311.

521 Sidlauskas, B. 2008. Continuous and arrested morphological diversification in sister clades of
522 characiform fishes: A phylomorphospace approach. Evolution 62:3135–3156.
523 Soares, D., and M. L. Niemiller. 2013. Sensory Adaptations of Fishes to Subterranean
524 Environments. BioScience 63:274–283.
525 Soares, D., M. Pluviose, and Y. Zhao. 2019. Ontogenetic development of the horn and hump of
526 the Chinese cavefish *Sinocyclocheilus furcodorsalis* (Cypriniformes: Cyprinidae). Environ
527 Biol Fish 102:741–746.
528 Staden, R. 1996. The staden sequence analysis package. Mol Biotechnol 5:233–241.
529 Strecker, U., V. H. Faúndez, and H. Wilkens. 2004. Phylogeography of surface and cave
530 *Astyanax* (Teleostei) from Central and North America based on cytochrome b sequence data.
531 Molecular Phylogenetics and Evolution 33:469–481.
532 Su, R., J. Yang, and G. Cui. 2003. Taxonomic review of the genus *Sinocrossocheilus wu*
533 (Teleostei: Cyprinidae), with a description of four new species. Zoological Studies 42:420–
534 430.
535 Tamura, K., G. Stecher, D. Peterson, A. Filipski, and S. Kumar. 2013. MEGA6: Molecular
536 Evolutionary Genetics Analysis Version 6.0. Molecular Biology and Evolution 30:2725–2729.
537 Thompson, J. D., T. J. Gibson, and D. G. Higgins. 2003. Multiple Sequence Alignment Using
538 ClustalW and ClustalX. Current Protocols in Bioinformatics 00: 2.3.1-2.3.22.
539 Wilkens, H. 2016. Genetics and hybridization in surface and cave *Astyanax* (Teleostei): a
540 comparison of regressive and constructive traits. Biol. J. Linn. Soc. 118:911–928.
541 Wilkens, H., and U. Strecker. 2017. Surface and cave populations of Mexican *Astyanax*. Pp. 37–
542 52 *in* Evolution in the Dark . Springer, Berlin, Heidelberg.

543 Yang, J., X. Chen, J. Bai, D. Fang, Y. Qiu, W. Jiang, H. Yuan, C. Bian, J. Lu, S. He, X. Pan, Y.
544 Zhang, X. Wang, X. You, Y. Wang, Y. Sun, D. Mao, Y. Liu, G. Fan, H. Zhang, X. Chen, X.
545 Zhang, L. Zheng, J. Wang, and L. Cheng. 2016. The *Sinocyclocheilus* cavefish genome
546 provides insights into cave adaptation. BMC Biology 14:1.
547 Yoshizawa, M. 2015. Behaviors of cavefish offer insight into developmental evolution: Evo-
548 Devo of cave fish behaviour. Mol. Reprod. Dev. 82:268–280.
549 Zhao, Y. 2006. Cavefishes: concept, diversity and research progress. Biodiversity Science
550 14:451.
551 Zhao, Y., and C. Zhang. 2009. Endemic Fishes of *Sinocyclocheilus* (Cypriniformes: Cyprinidae)
552 in China -Species diversity, cave adaptation, systematics and zoogeography. Science Press,
553 Beijing.
554

Main Figures

Fig. 1. (A) A specimen of *Sinocyclocheilus altishoulderus* indicating the position of 15 landmarks (red: larger points indicated by numbers 1-15) and 180 semi-landmarks (red: smaller point) used for the calculation of Procrustes coordinates and traditional linear measurements (SL: standard Length, ED: eye diameter and sED: standardized eye diameter) used in the geometric morphometric analyses. (B) **PCA showing the variation in body shape of the genus *Sinocyclocheilus* traced with eye morphology and habitat occupation.** PC1 and PC2 accounts for 32% and 17% of the variance respectively. A shift from the fusiform shape of the Normal-eyed surface forms to a more "boxy" form of the Micro-eyed and Blind forms is evident.

Fig. 2. Ancestral state reconstruction of morphology (Blind, Mico-eyed & Normal-eyed) on a time calibrated phylogeny. Posterior probabilities of node support also shown on the tree. **Maximum-likelihood reconstructions for the ancestral state of the eye-trait morphology (Blind, Micro and Normal-eyed morphs) on a time calibrated phylogeny.** A, B, C and D are four major clades. Posterior probabilities of node support values of 100% are indicated by *. Key events of *Sinocyclocheilus* evolution includes; at least three independent evolutionary events for Blind morphs; Blind, Micro-eyed and a few Normal-eyed species in clade B, with two cases of reversal from either Micro-eyed or Blind to Normal-eyed species.

Fig. 3. **Temporal patterns of body size and eye diameter in *Sinocyclocheilus* from the perspective of their eye trait related morphs.** The traitgrams suggests that the evolution of different morphs is attained by altering the allometric relationships between body size and eye

578 diameter. A. Traitgram of body size ; B. traitgram of eye size; C. Eye related morphs traced on
579 the phylomorphospace indicating clear separation of the three morphs in the morphospace.
580 (D)Habitat associations traced on the phylomorphospace showing species having eye diameter
581 <3mm and small to medium body sizes are obligate cave dwellers whereas species with eye
582 diameter >3mm can be Troglodytic, Troglophilic or Surface dwellers regardless of their body
583 size (E) Horn related morphs traced on the phylomorphospace indicating the presence of a horn
584 in smaller fish with reduced eye size. Horned species are Troglodytes.
585
586 **Fig. 4. Geophylogeny, the phylogeny laid across the geographic distribution of the species**
587 **considered in the analysis, with eye-related morphology, habitats, and horn-existence of the**
588 **species traced**. A pattern where basal, Normal-eyed, Troglodytic species are placed in the east,
589 predominantly Blind/Micro-eyed/Normal-Eyed, Troglodytic species in the center and Normal-
590 eyed, Surface dwelling species towards the western mountains is evident, indicating an East to
591 west dispersion of the genus *Sinocyclocheilus* across South and South Western China. Eye
592 specializations mostly occurred in Clade B, and horn evolution occurred exclusively in Clade B,
593 within the Central range of the *Sinocyclocheilus* distribution.
594
595

Main Tables:

Table 1. Model fit and estimated Brownian rate parameters for three traits (ED, sED and SL) in eye related morphs of *Sinocyclocheilus*. Multiple-rate models of evolution providing the best fit to the data for all three quantitative traits with ΔAIC >2.

Trait	Single rate model		Multiple rate model		ΔAIC
	AICc	AIC weights	AICc	AIC weights	
ED	253.9337	0.19991263	251.1600	0.800088	2.773681
sED	246.1558	0.004509138	235.3616	0.995491	10.794260
SL	538.3145	0.018806041	530.4053	0.981194	7.909184

Table 2. Model averaged rate parameters for the measured traits in eye related morphs of *Sinocyclocheilus.* Normal-eyed and Micro-Eyed species indicate similar evolutionary rates with marked shifts towards Blind species.

Trait	Model Averaged Rate		
	Blind	Micro-eyed	Normal-eyed
SL	45.3506	1597.9230	1275.5080
ED	11.3935	2.9984	3.8872
sED	24.9441	1.6925	2.2773

610 **Fig.1**

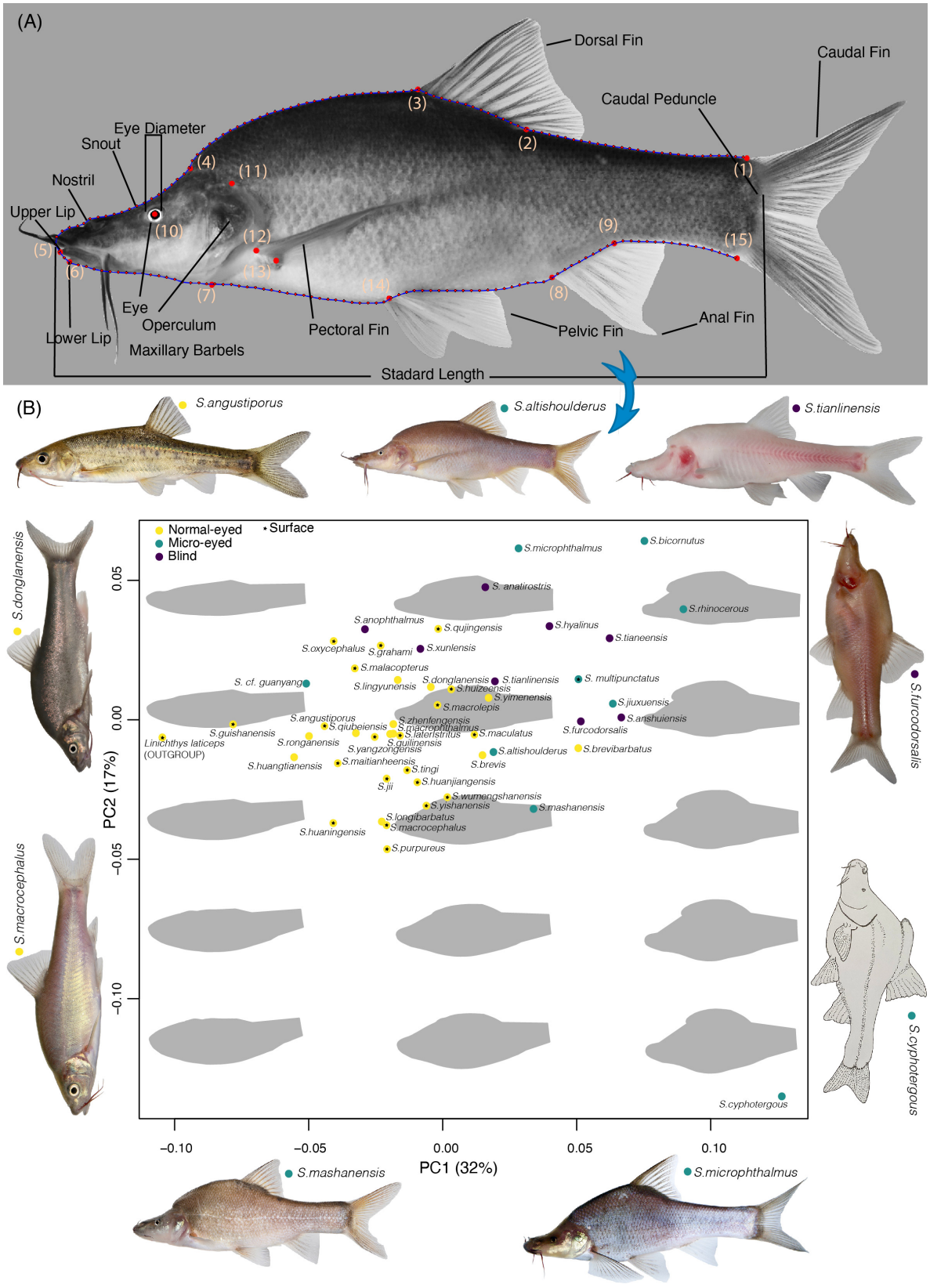

611

612 **Fig.2.**

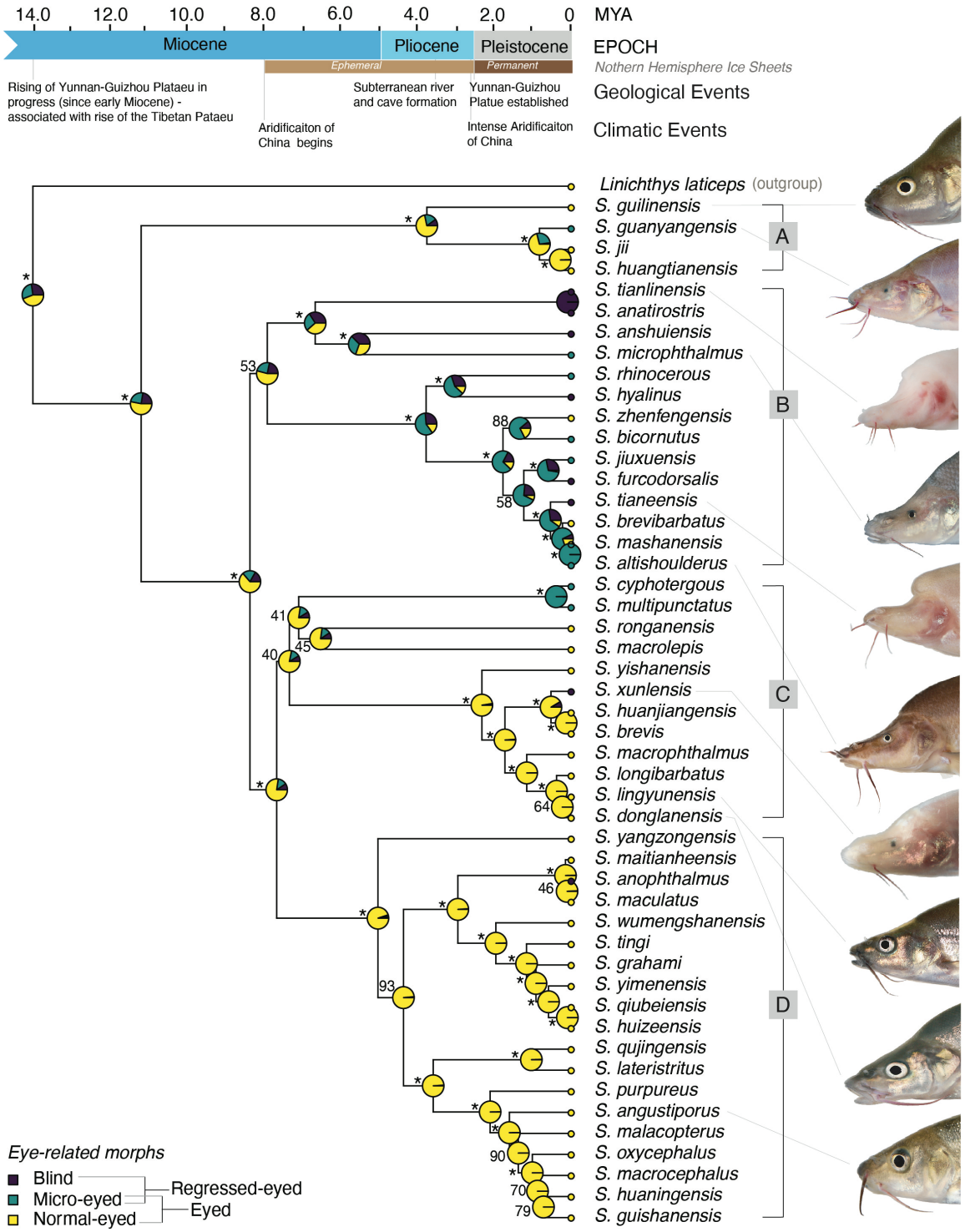

613

Fig. 3.

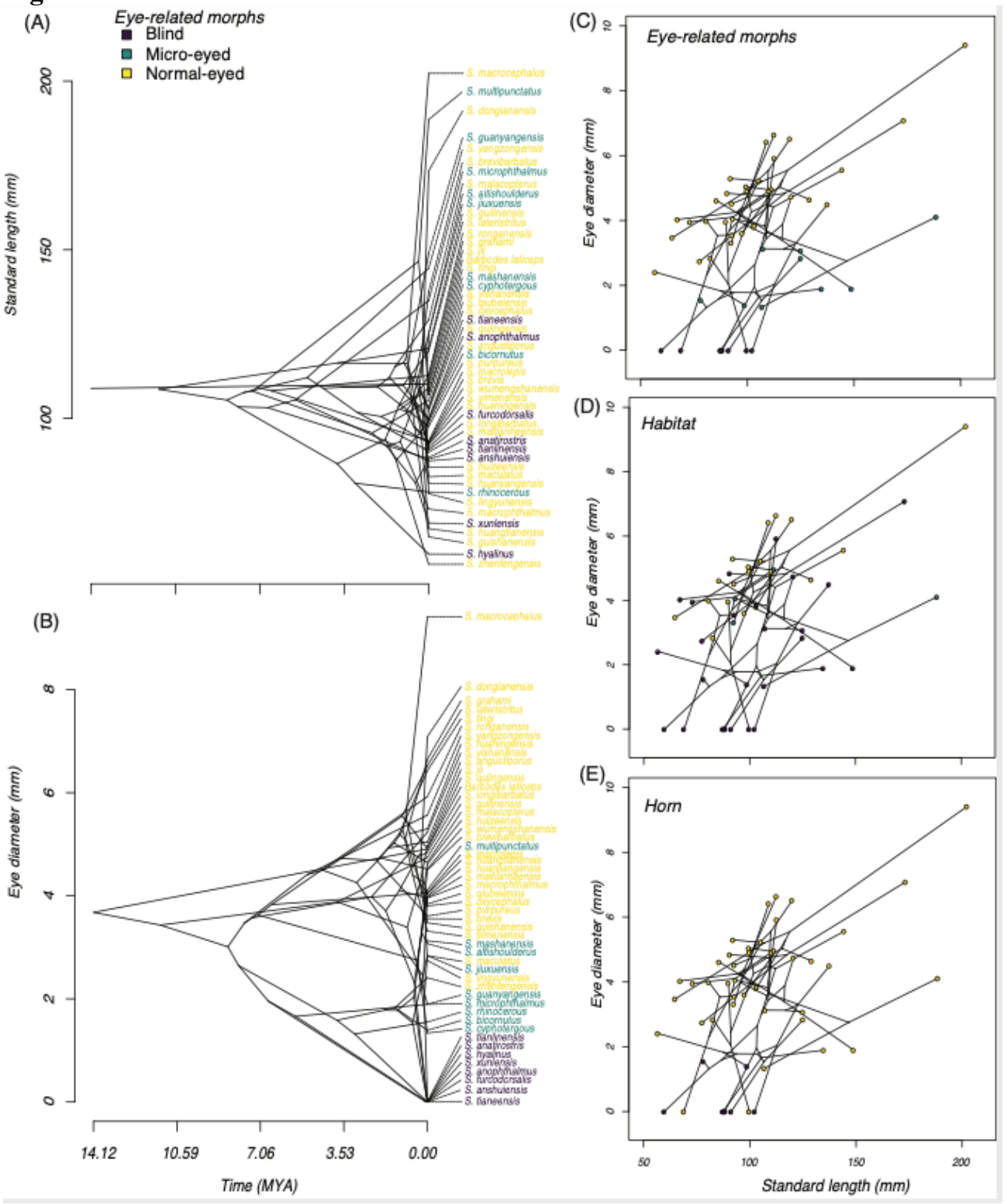

Fig.4.

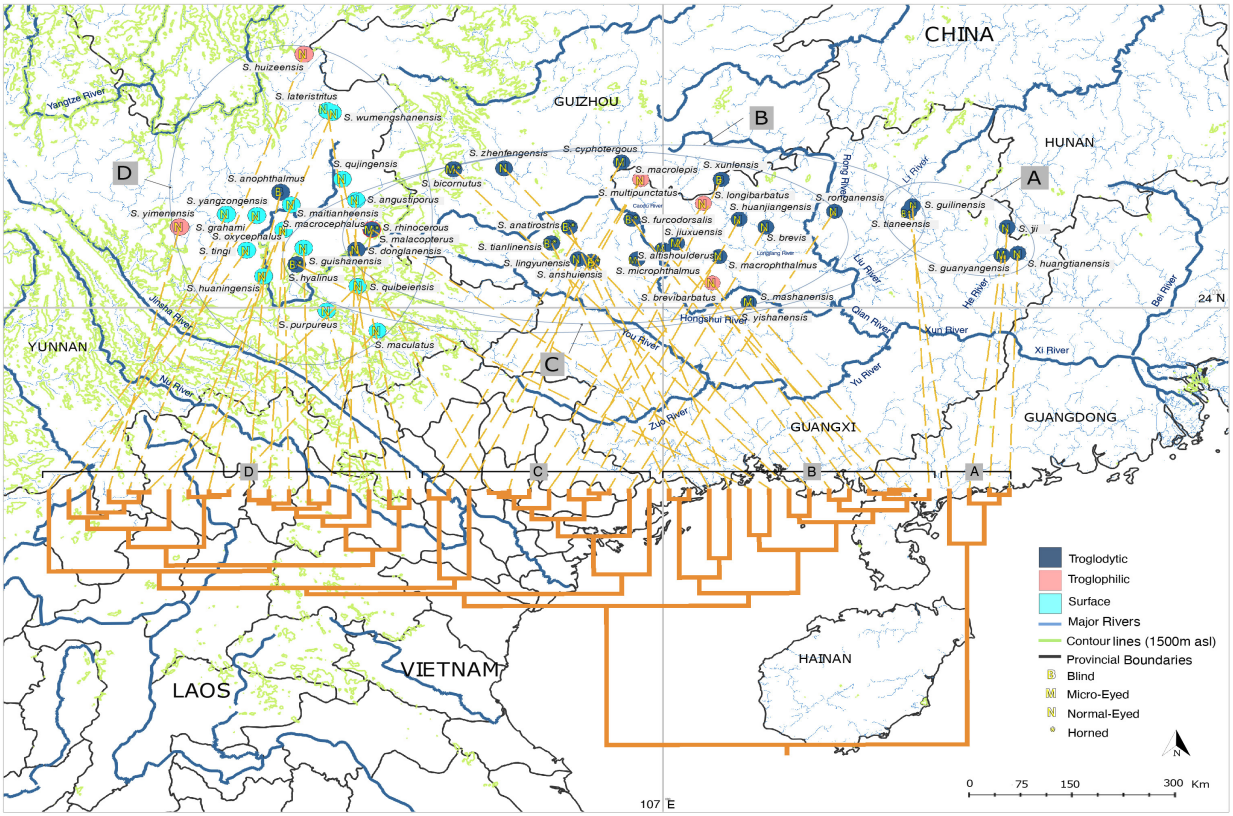

Supplementary Information:

640 Fig. S1. Maximum-likelihood reconstructions for the ancestral states of the habitat occupation
641 (Troglodytic, Troglophilic and Surface) on the phylogeny of the genus *Sinocyclocheilus*.

642

643 Fig. S2. Maximum-likelihood reconstructions for the ancestral state of the horn related trait
644 (presence/absence of horn) on the phylogeny of the genus *Sinocyclocheilus*.

645

646 Table S1. Species information and GenBank accession numbers of two mtDNA fragments
647 (*NADH4* and *cytb*) of 39 *Sinocyclocheilus* species. The information of the outgroup species
648 *Linichthys laticeps* (Cyprinidae) is also indicated along with calculated standard length (SL), eye
649 diameter (ED), standard eye diameter (sED), discrete trait categories related to eye morphology
650 (Blind, Micro-eyed, Normal eyed), presence or absence of a horn and habitat occupation
651 (Troglodytic, Troglophilic and surface) for all species used in the analysis. Accession numbers
652 indicated as XXXX will be accessible upon the acceptance of the manuscript.

Species name	**SL**	**ED**	**SED**	**CYTB**	**NADH4**	**Morph**	**Habitat**	**Horn**
Linichthys laticeps	110.20	4.91	4.45	AY854739	AY854796	Normal-eyed	Surface	Absent
S. altishoulderus	125.10± 16.74	3.07±0.35	2.46	AY854724	AY854781	Micro-eyed	Troglodytic	Absent
S. anatirostris	88.40	0.00	0	AY854708	AY854765	Blind	Troglodytic	Present
S. angustiporus	99.57±19.79	5.05±0.77	5.07	AY854702	AY854759	Normal-eyed	Surface	Absent
S. anophthalmus	99.80	0.00	0	AY854715	AY854772	Blind	Troglodytic	Absent
S. anshuiensis	87.40	0.00	0	NC_027169	NC_039769	Blind	Troglodytic	Present
S. bicornutus	98.80	1.39	1.41	AY854730	AY854787	Micro-eyed	Troglodytic	Present
S. brevibarbatus	137.55±18.17	4.50±0.84	3.27	XXXX	-	Normal-eyed	Troglophilic	Absent
S. brevis	92.91±6.39	3.55±0.14	3.83	XXXX	-	Normal-eyed	Troglodytic	Absent
S. guanyangensis	148.92±7.39	1.90±1.14	1.27	AY854711	AY854768	Micro-eyed	Troglodytic	Absent
S. cyphotergous	106.95±13.08	1.34±0.61	1.25	AB196440	-	Micro-eyed	Troglodytic	Absent
S. donglanensis	173.37±15.94	7.09±0.69	4.09	AY854709	AY854766	Normal-eyed	Troglodytic	Absent
S. furcodorsalis	91.29±16.36	0.00	0	AY854694	AY854751	Blind	Troglodytic	Present
S. grahami	112.60	6.64	5.9	XXXX	-	Normal-eyed	Surface	Absent

S. guilinensis	120.68±15.04	4.74±0.33	3.93	XXXX	-	Normal-eyed	Troglodytic	Absent
S. guishanensis	64.90	3.48	5.35	AY854722	AY854779	Normal-eyed	Surface	Absent
S. huangtianensis	67.32±20.48	4.03±0.72	5.99	XXXX	-	Normal-eyed	Troglodytic	Absent
S. huaningensis	92.20	5.30	5.75	AY854718	AY854775	Normal-eyed	Surface	Absent
S. huanjiangensis	80.79±17.68	3.99±0.45	4.94	XXXX	-	Normal-eyed	Troglodytic	Absent
S. huizeensis	85.60	4.61	5.39	NC_044072	NC_039769	Normal-eyed	Troglophilic	Absent
S. hyalinus	59.80±28.43	0.00	0	AY854721	AY854778	Blind	Troglodytic	Present
S. jii	111.43±17.21	4.97±0.47	4.46	AY854727	AY854784	Normal-eyed	Troglodytic	Absent
S. jiuxuensis	125.10	2.84	2.27	AY854736	AY854793	Micro-eyed	Troglodytic	Absent
S. lateristritus	120.00	6.52	5.43	AY854703	AY854760	Normal-eyed	Surface	Absent
S. lingyunensis	77.69±9.35	2.75±0.60	3.53	AY854691	AY854748	Normal-eyed	Troglodytic	Absent
S. longibarbatus	90.63±1.82	4.84±0.24	5.34	AY854714	AY854771	Normal-eyed	Troglophilic	Absent
S. macrocephalus	202.30	9.42	4.65	AY854683	AY854740	Normal-eyed	Surface	Absent
S. macrolepis	93.30	4.06	4.35	AY854729	AY854786	Normal-eyed	Troglophilic	Absent
S. macrophthalmus	73.16±11.50	3.96±0.71	5.41	AY854735	AY854792	Normal-eyed	Troglodytic	Absent
S. maculatus	82.70	2.84	3.43	EU366193	EU366183	Normal-eyed	Surface	Absent
S. maitianheensis	90.00	3.96	4.4	AY854710	AY854767	Normal-eyed	Surface	Absent
S. malacopterus	129.20	4.65	3.6	AY854697	AY854754	Normal-eyed	Surface	Absent
S. mashanensis	107.36±5.72	3.13±0.34	2.91	XXXX	-	Micro-eyed	Troglodytic	Absent
S. microphthalmus	134.89±10.51	1.89±0.38	1.4	AY854687	AY854744	Micro-eyed	Troglodytic	Absent
S. multipunctatus	188.60	4.11	2.18	AY854712	AY854769	Micro-eyed	Troglophilic	Absent
S. oxycephalus	103.10	3.80	3.69	AY854685	AY854742	Normal-eyed	Surface	Absent
S. purpureus	97.60	3.61	3.7	EU366194	EU366177	Normal-eyed	Surface	Absent
S. qiubeiensis	103.30	3.84	3.72	EU366195	EU366181	Normal-eyed	Surface	Absent
S. qujingensis	99.90	4.91	4.92	AY854719	AY854776	Normal-eyed	Surface	Absent
S. rhinocerous	78.20	1.55	1.98	AY854720	AY854777	Micro-eyed	Troglodytic	Present
S. ronganensis	112.72	5.92	5.25	NC_032385	NC_039769	Normal-eyed	Troglodytic	Absent
S. tianeensis	102.34±12.43	0.00	0	AY854717	AY854774	Blind	Troglodytic	Present
S. tianlinensis	87.96±27.97	0.00	0	XXXX	-	Blind	Troglodytic	Present
S. tingi	109.00	6.42	5.89	AY854701	AY854758	Normal-eyed	Surface	Absent
S. wumengshanensis	92.80	4.52	4.87	NC_039769	NC_039769	Normal-eyed	Surface	Absent
S. xunlensis	69.01±21.44	0.00	0	EU366187	EU366184	Blind	Troglodytic	Absent
S. yangzongensis	144.50	5.56	3.85	AY854725	AY854782	Normal-eyed	Surface	Absent
S. yimenensis	92.50	3.31	3.58	EU366192	EU366179	Normal-eyed	Troglophilic	Absent
S. yishanensis	105.34±8.15	5.23±0.23	4.97	XXXX	-	Normal-eyed	Troglodytic	Absent

S. zhenfengensis	56.78	2.41	4.24	MK610342	MK610347	Normal-eyed	Troglodytic	Absent

653

654 Table S2. Information of digitized images used in the morphometric geometric analysis. Table
655 indicates the voucher number of the specimen used for the analysis and the reference from which
656 the image was obtained. Images photographed during the current study are also indicated with
657 voucher numbers stated as GXUXXX (GXU: Guangxi University, China).

658

Species name	Reference	Voucher #
Linichthys laticeps	Zhang, E., and F. Fang. 2005. Linichthys: A New Genus of Chinese Cyprinid Fishes (Teleostei: Cypriniformes). Copeia 2005:61–67.	*IHB 78X6242*
S. altishoulderus	Guangxi University (this study).	*GXU001, GXU002, GXU003*
S. anatirostris	Romero, A., Y. Zhao, and X. Chen. 2009. The Hypogean fishes of China. Environ Biol Fish 86:211–278.	*IHB 84VII255,*
S. angustiporus	Guangxi University (this study).	*GXU007, GXU008 , GXU009*
S. anophthalmus	Romero, A., Y. Zhao, and X. Chen. 2009. The Hypogean fishes of China. Environ Biol Fish 86:211–278.	*KIZ 865949*
S. anshuiensis	Xi, G., W. Tie-Jun, W. Mu-Lan, and Y. Jian. 2013. A new blind barbine species, *Sinocyclocheilus anshuiensis* sp. nov.(Cypriniformes: Cyprinidae) from Guangxi, China. Kunming Institute of Zoology, Chinese Academy of Sciences.	*12070276*
S. bicornutus	Romero, A., Y. Zhao, and X. Chen. 2009. The Hypogean fishes of China. Environ Biol Fish 86:211–278.	*IHB 12209043-9o5o241*
S. brevibarbatus	Guangxi University (this study).	*GXU010, GXU011, GXU012*
S. brevis	Guangxi University (this study). Romero, A., Y. Zhao, and X. Chen. 2009. The Hypogean fishes of China. Environ Biol Fish 86:211–278.	*GXU013, GXU014* *IHB12209033-*

		87087496
S. cyphotergous	Romero, A., Y. Zhao, and X. Chen. 2009. The Hypogean fishes of China. Environ Biol Fish 86:211–278. Huang, J., A. Gluesenkamp, D. Fenolio, Z. Wu, and Y. Zhao. 2017. Neotype designation and redescription of *Sinocyclocheilus cyphotergous* (Dai) 1988, a rare and bizarre cavefish species distributed in China (Cypriniformes: Cyprinidae). Environ Biol Fish 100:1483–1488.	*IHB 12209040* *ASIZB 204678*
S. donglanensis	Guangxi University (this study).	*GXU015, GXU016, GXU017*
S. furcodorsalis	Guangxi University (this study).	*GXU018, GXU019, GXU020*
S. grahami	Romero, A., Y. Zhao, and X. Chen. 2009. The Hypogean fishes of China. Environ Biol Fish 86:211–278.	*ASIZB 03496*
S. guanyangensis	Guangxi University (this study).	*GXU004,GXU005, GXU006*
S. guilinensis	Guangxi University (this study).	*GXU021, GXU022, GXU023*
S. guishanensis	Romero, A., Y. Zhao, and X. Chen. 2009. The Hypogean fishes of China. Environ Biol Fish 86:211–278.	*Li980514005*
S. huangtianensis	Guangxi University (this study).	*GXU024, GXU025, GXU026*
S. huaningensis	Romero, A., Y. Zhao, and X. Chen. 2009. The Hypogean fishes of China. Environ Biol Fish 86:211–278.	*ASIZB79228*
S. huanjiangensis	Guangxi University (this study).	*GXU027, GXU028, GXU029*
S. huizeensis	Cheng, C., P. Xiao-Fu, C. Xiaoyong, J. Li, L. Ma, and J. Yang. 2015. A new species of the genus *Sinocyclocheilus* (Teleostei:Cypriniformes), from Jinshajiang Drainage, Yunnan, China. Cave Research 1:1–4.	*KIZ2013001246*
S. hyalinus	Romero, A., Y. Zhao, and X. Chen. 2009. The Hypogean fishes of China. Environ Biol Fish 86:211–278.	*KIZ916001* *Photograph in life*

	You, H., C. Xiaoyong, X. Ti-Qao, and Y. Jun-Xing. 2013. Three-dimensional morphology of the *Sinocyclocheilus hyalinus* (Cypriniformes : Cyprinidae) horn based on synchrotron X-ray microtomography. Zoological research 34:128–134.	
S. jii	Romero, A., Y. Zhao, and X. Chen. 2009. The Hypogean fishes of China. Environ Biol Fish 86:211–278. Baradi, W., Z. Yahui, Z. Chunguang, D. Rongji, and A. Abdul. 2013. Anatomical Studies of the Olfactory Epithelium of Two Cave Fishes *Sinocyclocheilus jii* and *S. furcodorsalis* (Cypriniformes: Cyprinidae) from China. Pakistan Journal of Zoology 45:1091 – 1101.	*ASIZB62726* *Photograph in life*
S. jiuxuensis	Romero, A., Y. Zhao, and X. Chen. 2009. The Hypogean fishes of China. Environ Biol Fish 86:211–278.	*ASIZB102260*
S. lateristritus	Romero, A., Y. Zhao, and X. Chen. 2009. The Hypogean fishes of China. Environ Biol Fish 86:211–278.	*IHB12209036-865027*
S. lingyunensis	Guangxi University (this study). Romero, A., Y. Zhao, and X. Chen. 2009. The Hypogean fishes of China. Environ Biol Fish 86:211–278.	*GXU030* *ASIZB 73038*
S. longibarbatus	Guangxi University (this study).	*GXU031, GXU032, GXU033*
S. macrocephalus	Romero, A., Y. Zhao, and X. Chen. 2009. The Hypogean fishes of China. Environ Biol Fish 86:211–278.	*IHB12209012-662001*
S. macrolepis	Romero, A., Y. Zhao, and X. Chen. 2009. The Hypogean fishes of China. Environ Biol Fish 86:211–278.	*IHB12209035-87IV457*
S. macrophthalmus	Guangxi University (this study).	*GXU034,GXU035,GXU036*
S. maculatus	Romero, A., Y. Zhao, and X. Chen. 2009. The Hypogean fishes of China. Environ Biol Fish 86:211–278.	*Li870808001*

S. maitianheensis	Romero, A., Y. Zhao, and X. Chen. 2009. The Hypogean fishes of China. Environ Biol Fish 86:211–278.	*IHB12209039-874001*
S. malacopterus	Romero, A., Y. Zhao, and X. Chen. 2009. The Hypogean fishes of China. Environ Biol Fish 86:211–278.	*KIZ775831*
S. mashanensis	Guangxi University (this study).	*GXU037, GXU038, GXU039*
S. microphthalmus	Guangxi University (this study).	*GXU040, GXU041, GXU042*
S. multipunctatus	Romero, A., Y. Zhao, and X. Chen. 2009. The Hypogean fishes of China. Environ Biol Fish 86:211–278.	*ASIZB73000*
S. oxycephalus	Romero, A., Y. Zhao, and X. Chen. 2009. The Hypogean fishes of China. Environ Biol Fish 86:211–278.	*IHB12209013-652047*
S. purpureus	Romero, A., Y. Zhao, and X. Chen. 2009. The Hypogean fishes of China. Environ Biol Fish 86:211–278.	*IHB12209015-731004*
S. qiubeiensis	Romero, A., Y. Zhao, and X. Chen. 2009. The Hypogean fishes of China. Environ Biol Fish 86:211–278.	*Li990527002*
S. qujingensis	Romero, A., Y. Zhao, and X. Chen. 2009. The Hypogean fishes of China. Environ Biol Fish 86:211–278.	*ASIZB78790*
S. rhinocerous	Romero, A., Y. Zhao, and X. Chen. 2009. The Hypogean fishes of China. Environ Biol Fish 86:211–278.	*ASIZB93907*
S. ronganensis	FuGuang, L., H. Jie, L. Xia, L. Tong, and W. YanHong. 2016. *Sinocyclocheilus ronganensis* Luo, Huang et Wen sp. nov., a new species belonging to *Sinocyclocheilus* Fang from Guangxi (Cypriniformes: Cyprinidae). Guangxi Academy of Agricultural Sciences 47:650–655.	*20151114001*
S. tianeensis	Guangxi University (this study).	*GXU043, GXU044, GXU045*
S. tianlinensis	Guangxi University (this study).	*GXU052, GXU053, GXU054*
S. tingi	Romero, A., Y. Zhao, and X. Chen. 2009. The Hypogean fishes of China. Environ Biol Fish 86:211–278.	*ASIZB60227*

S. wumengshanensis	Romero, A., Y. Zhao, and X. Chen. 2009. The Hypogean fishes of China. Environ Biol Fish 86:211–278.	*KIZ82100006*
S. xunlensis	Guangxi University (this study).	*GXU046, GXU047, GXU048*
S. yangzongensis	Romero, A., Y. Zhao, and X. Chen. 2009. The Hypogean fishes of China. Environ Biol Fish 86:211–278.	*KIZ6351069*
S. yimenensis	Romero, A., Y. Zhao, and X. Chen. 2009. The Hypogean fishes of China. Environ Biol Fish 86:211–278.	*Li030509009*
S. yishanensis	Romero, A., Y. Zhao, and X. Chen. 2009. The Hypogean fishes of China. Environ Biol Fish 86:211–278.	*GXU049, GXU050, GXU051*
S. zhenfengensis	Liu, T., H. Q. Deng, L. Ma, N. Xiao, and J. Zhou. 2018. *Sinocyclocheilus zhenfengensis* , a new cyprinid species (Pisces: Teleostei) from Guizhou Province, Southwest China. J Appl Ichthyol 34:945–953.	*GZNU20120701001*

659

660 Table S3. Calculated Principal Component values (PC1, PC2 and PC3) of all the specimens used

661 in the current analysis

Spname	PC1val	PC2val	PC3cal
Linichthys laticeps	0.1069618	-0.006044939	-0.032010383
S. altishoulderus	-0.01804998	-0.010081536	-0.046423134
S. anatirostris	-0.01766386	0.046175863	0.051169448
S. angustiporus	0.04334953	-0.002675304	0.034186136
S. anophthalmus	0.02908059	0.031606384	0.00917709
S. anshuiensis	-0.06639039	-0.000250595	-0.004873197
S. bicornutus	-0.07667729	0.060886565	0.012973894
S. brevibarbatus	-0.05048176	-0.011045867	0.006805293
S. brevis	-0.0142754	-0.011768784	-0.001763996

S. guanyangensis	-4.38E-05	0.015156895	-0.025200906
S. cyphotergous	-0.1220022	-0.139796596	0.008525168
S. donglanensis	0.004198408	0.013428914	-0.021746042
S. furcodorsalis	-0.050741	-0.000898602	-0.044412032
S. grahami	0.02231859	0.026236004	0.022098623
S. guilinensis	0.01963493	-0.0033727	-0.023009295
S. guishanensis	0.07886827	0.00257981	-0.059167855
S. huangtianensis	0.05562456	-0.011114954	0.021111628
S. huaningensis	0.04117411	-0.037450418	0.031061221
S. huanjiangensis	0.009958768	-0.021868616	0.007063138
S. huizeensis	-0.003779219	0.010286192	0.031012201
S. hyalinus	-0.03974731	0.030183657	0.039671171
S. jii	0.02155773	-0.019701057	-0.005284772
S. jiuxuensis	-0.06337799	0.004932247	-0.008080491
S. lateristritus	0.01609448	-0.006156199	0.021918263
S. lingyunensis	0.01666848	0.015544267	0.002003128
S. longibarbatus	0.0238826	-0.037134912	0.007645544
S. macrocephalus	0.0223646	-0.03930768	0.034945546
S. macrolepis	0.002586613	0.0056233	-0.005281302
S. macrophthalmus	0.01921085	-0.004423179	0.011957836
S. maculatus	-0.01164108	-0.003338214	-0.043022304
S. maitianheensis	0.04058493	-0.015399253	-0.004022456
S. malacopterus	0.03369873	0.016341474	0.002649988
S. mashanensis	-0.03299028	-0.033529198	-0.005547116
S. microphthalmus	-0.02936266	0.061223556	-0.040563771
S. multipunctatus	-0.05126049	0.014657848	-0.010821531

S. oxycephalus	0.04140438	0.030989746	-0.036348165
S. purpureus	0.02288238	-0.045035385	-0.018448807
S. qiubeiensis	0.03248934	-0.003880679	0.012191068
S. qujingensis	0.000644406	0.033555511	0.046291334
S. rhinocerous	-0.08985807	0.03649387	-0.020510521
S. ronganensis	0.05067357	-0.004282673	-0.02013066
S. tianeensis	-0.06234116	0.02827463	-0.030564848
S. tianlinensis	-0.01905521	0.012948686	-0.00406653
S. tingi	0.01508119	-0.019031787	-0.002178747
S. wumengshanensis	-0.000171791	-0.027155405	0.003238896
S. xunlensis	0.008420042	0.022462118	0.047598226
S. yangzongensis	0.02622031	-0.003887167	-0.006000758
S. yimenensis	-0.01762049	0.008265106	0.019258774
S. yishanensis	0.007505367	-0.029610044	-0.01952727
S. zhenfengensis	0.01938822	-0.002301361	0.003044235

678 **Fig.S1.**

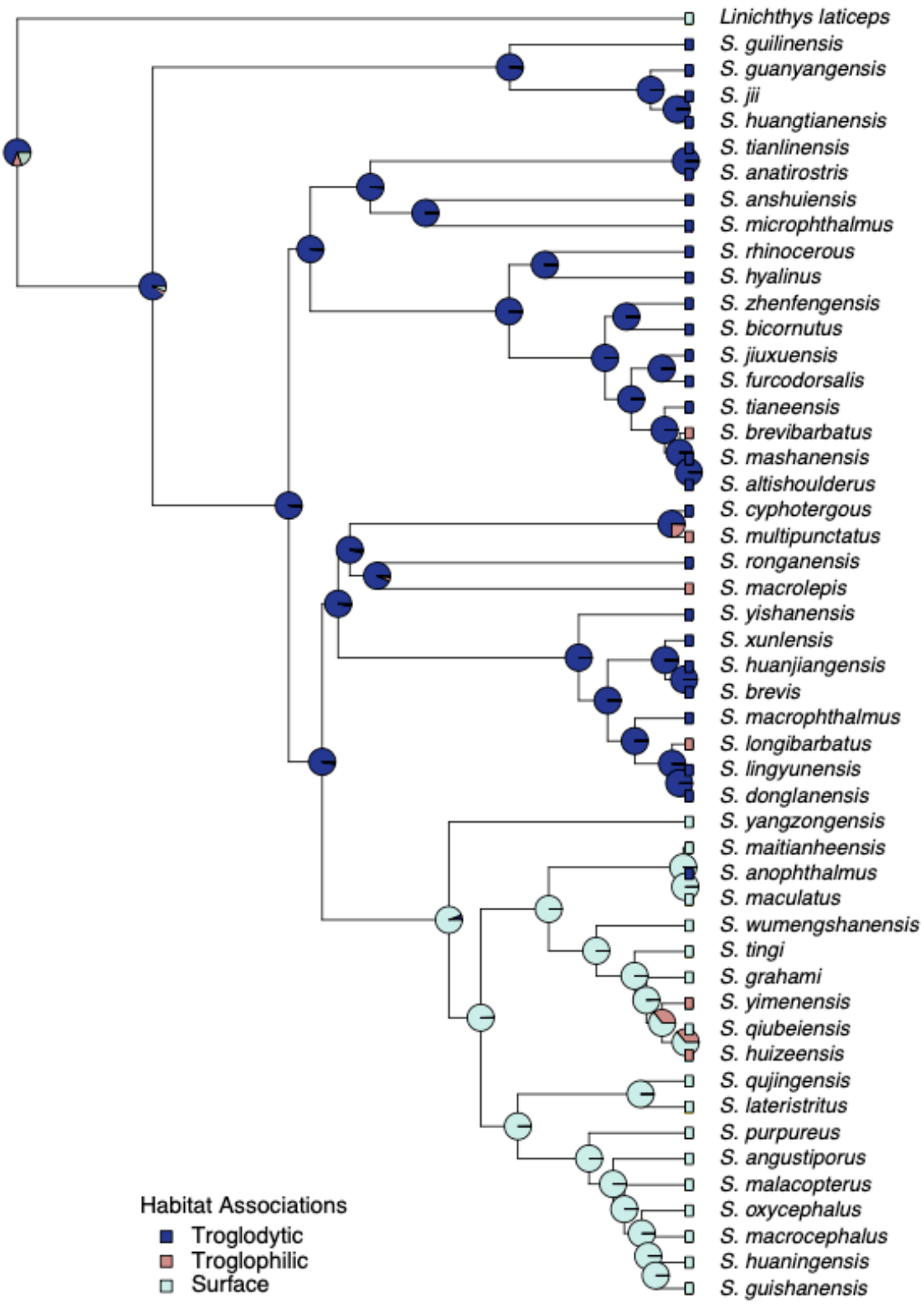

679
680

681 **Fig.S2.**

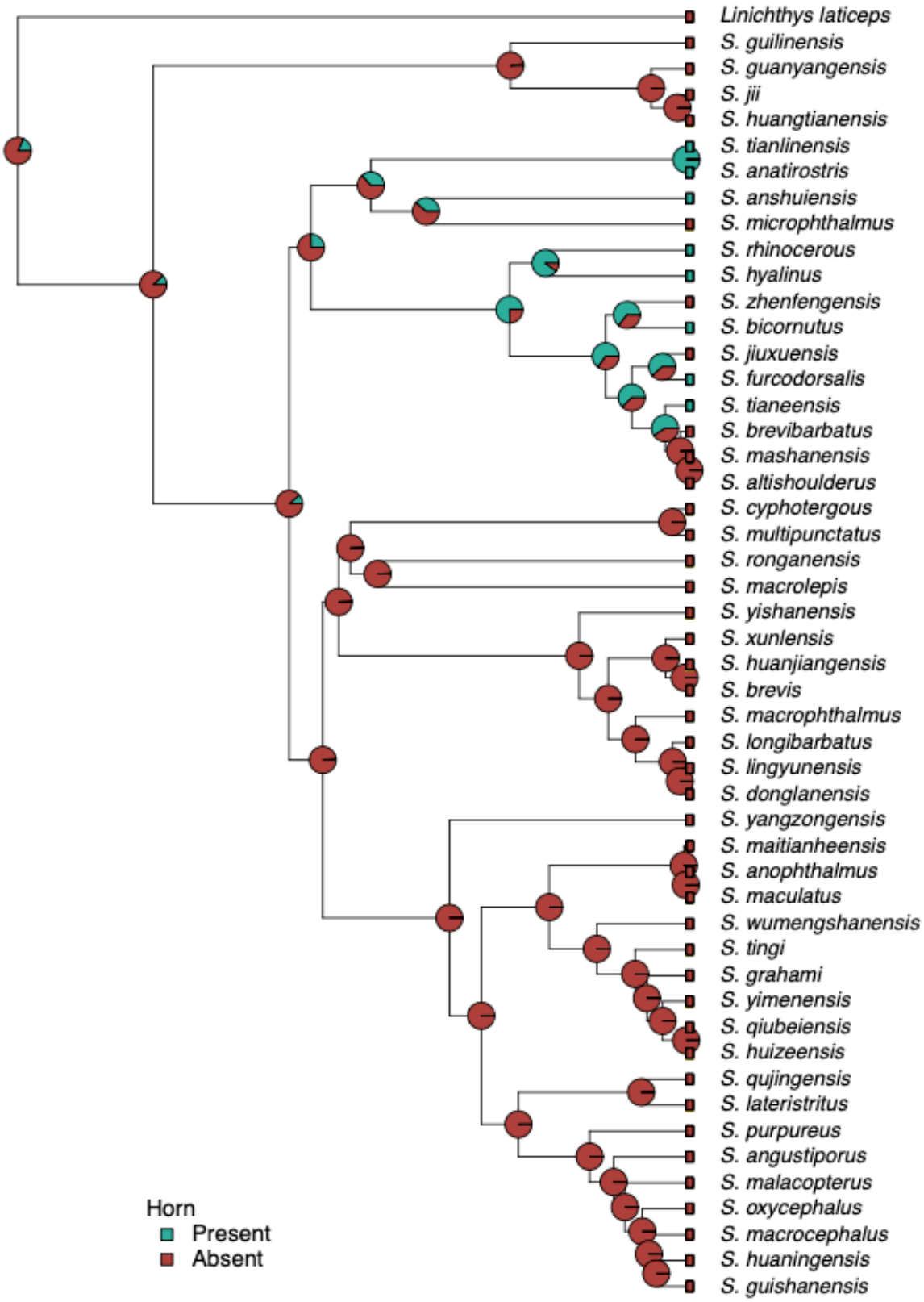

682